Diammonium glycyrrhizinate lipid ligand ameliorates lipopolysaccharide-induced acute lung injury by modulating vascular endothelial barrier function

Mei-Mei Liu
Anhui Medical University
Jin Zhou
Anhui Medical University
Dan Ji
Anhui Medical University
Jun Yang
Anhui Medical University
Yan-Ping Huang
Anhui Medical University
Qi Wang (41722315@qq.com)
Anhui Medical University https://orcid.org/0000-0003-1203-9255

Research

Keywords: diammonium glycyrrhizinate lipid ligand, inflammatory infiltration, VE-Cadherin, tight junction protein

Posted Date: January 28th, 2020

DOI: https://doi.org/10.21203/rs.2.22082/v1

Version of Record: A version of this preprint was published at Experimental and Therapeutic Medicine on January 29th, 2021. See the published version at https://doi.org/10.3892/etm.2021.9734.

Abstract

Background: The present study investigated the attenuating effect of diammonium glycyrrhizinate lipid ligand (DGLL) on acute lung injury (ALI) and pulmonary edema induced by lipopolysaccharide (LPS) in rats.

Methods: Rat ALI model was established by LPS (10 mg/kg) intraperitoneal injection, and DGLL (30, 60, 120 mg/kg) was administrated orall 1 hour before LPS infusion. Six hours after LPS stimulation, lung injury was evaluated by histological staining. Pulmonary edema was evaluated by lung wet-dry weight ratio, the protein concentration of bronchoalveolar lavage fluid (BALF), and the evans blue (EB) extravasation in lung tissues. The expression of cytokines and adhesion molecules in lung tissues were detected by ELISA method. The myeloperoxidase (MPO) expression was detected by immunohistochemical staining. Western blot was used to detect the expression changes of the proteins associated with pulmonary inflammation and microvascular permeability.

Results: DGLL significantly inhibited LPS induced ALI, manifested as attenuation of MPO positive cells and TNF-α, IL-6, ICAM-1 expression in rat lung tissue. In addition, DGLL abrogated LPS-induced pulmonary edema, decreased the protein concentration in BALF and EB extravasation. Meanwhile, DGLL inhibited the degradation of vascular endothelial cadherin (VE-Cadherin) and tight junction protein, including ZO-1, Occludin, and JAM-1.

Conclusions: DGLL has an inhibitory effect on LPS-induced rat ALI, which is related to the inhibition of inflammatory cell infiltration and microvascular barrier disruption. These results provide a theoretical basis for DGLL in the potential clinical treatment of ALI.

Background

Acute lung injury (ALI) referred to the pathological features of pulmonary edema and atelectasis caused by diffuse alveolar-capillary membrane damage, manifested as respiratory distress and refractory hypoxemia. ALI is one the common serious pathological process in many diseases, such as severe infection, trauma, shock, and harmful gas inhalation. Acute respiratory distress syndrome (ARDS) was a severe form of ALI that can rapidly developed into multiple organ failure with a poor prognosis [1]. Anti-inflammatory treatment was currently the main method for clinical treatment of ALI, however, clinical trials have found that hormonal drugs had an unforeseen side effects in clinical use, and could not reduce the mortality rate of ALI patients, even though a significant inhibitory effect on the inflammatory response during ALI was obvious [2]. Other inhaled anti-asthmatic drugs, such as, activated protein C, albuterol, surfactants have all been withdrew due to poor clinical efficacy or side effects. In recent years, people had a new understanding of the pathogenesis and pathophysiological process of ALI/ARDS. Clinical and experimental studies have shown that pulmonary capillary barrier injury, followed by increased pulmonary edema were the most important pathological lesion and pathological basis in the

early stages of ALI/ARDS [3]. However, there was still a lack of effective therapeutic drugs and therapeutic measures for the increase of pulmonary microvascular permeability [4].

The diammonium glycyrrhizinate lipid ligand (DGLL), also known as Tianqing Ganping (TPG), was the third-generation extract of the active ingredient of Glycyrrhiza uralensis. As a medicine for antitussive and antiasthmatic, the traditional Chinese medicine licorice has been widely used as one of the active components in compound Chinese preparation for treating respiratory infections and acute lung injury, such as Mahuang decoction and Maxing Shigan decoction, etc [5, 6]. Modern clinical observations have also found that glycyrrhizin alone or combination with other drugs could effectively reduce lung injury, improve alveolar gas exchange, and inhibit pulmonary inflammation [7–9]. Our previous studies have shown that DGLL had a significant inhibitory effect on inflammatory responses and can inhibit the inflammatory response of non-alcoholic fatty liver in rats, including suppression of inflammatory mediator expression, inhibition of leukocyte adhesion, infiltration, and peroxide release. However, whether DGLL could improve pulmonary edema, the key link in ALI, and its mechanism have not yet been fully elucidated. Therefore, the present study investigated the effects and underlying mechanisms of DGLL on acute lung injury and pulmonary edema induced by lipopolysaccharide (LPS) in rat.

Results

1. DGLL inhibits LPS-induced rat ALI and pulmonary inflammation

HE staining showed that the rat lung structure was complete, with clear alveolar space, and no edema and inflammatory cell infiltration in alveolar septa in Sham group (Fig. 1A, a1). In contrast, in LPS group, an obvious edema and thickening was occurred in pulmonary interstitial, accompanied by alveolar atrophy and increased inflammatory cell infiltration (Fig. 1A, a2). Interestingly, DGLL pre-treatment group significantly aborgated LPS-induced ALI and recovered alveolar structure, which was more pronounced in 60 mg/kg and 120 mg/kg dose groups (Fig. 1A, a3-a5).

Immunohistochemistry examination showed that compared with Sham group (Fig. 1B, b1), the myeloperoxidase (MPO) positive cells staining in rat pulmonary tissue after LPS stimulation significantly increased (Fig. 1B, b2). The MPO positive staining in DGLL pre-treatment groups was significantly weaker than that in LPS group, and the number of MPO positive cells was significantly decreased in a dose-dependent manner (Fig. 1B, b3-b5), indicating that DGLL inhibited LPS-induced leukocyte infiltration in rat pulmonary tissue.

2. DGLL inhibits LPS-induced cytokine and adhesion molecules expression in rat lung tissue

ELISA showed that LPS induced a remarkable increased of inflammatory cytokines TNF-α and IL-1β expression in lung tissue compared to Sham group. Expectedly, both pretreatment with 60 mg/kg and 120 mg/kg of DGLL significantly inhibited LPS-induced increase in inflammatory factor levels in lung tissue while the pretreatment of 30 mg/kg DGLL had no significant effect (Fig. 2A and 2B). Similarly, western blot analysis suggested that, after 6 h of LPS stimulation, the lung tissue endothelial adhesion

molecule ICAM-1 levels were significantly increased and pretreatment of 60 mg/kg and 120 mg/kg DGLL also significantly inhibited LPS-induced up-regulation of ICAM-1 levels in rat lung tissue (Fig. 2C).

3. DGLL inhibits LPS-induced increase in pulmonary microvascular permeability and pulmonary edema

Compared with Sham group, lung tissue edema significantly increased after LPS induction for 6 hours, manifested as a significant increase in wet-to-dry weight ratio of rat lung tissue (Fig. 3A). Meanwhile, after LPS stimulation, the extravasation of evans blue (EB) in the lung tissue and the protein content in the bronchoalveolar lavage fluid (BALF) were significantly higher than those in Sham group (Fig. 3B, Fig. 3C), indicating that LPS can significantly impair the integrity of the pulmonary vascular endothelial and alveolar epithelial barrier. Surprisingly, in the DGLL 60 mg/kg and 120 mg/kg dose groups, all of the aforementioned changes, including lung wet/dry weight ratio, EB extravasation, and BALF protein concentration were significantly lower than those in LPS group, suggesting that pre-treatment with DGLL significantly inhibited LPS-induced pulmonary edema and increase of pulmonary microvascular permeability (Fig. 3).

4. DGLL inhibits LPS-induced phosphorylation and degradation of VE-cadherin in lung tissue

Western blot analysis showed that phosphorylation of the adhesion junction protein VE-cadherin (p-VE-cadherin) in the lung tissue was significantly higher than Sham group 6 hours after LPS induction (Fig. 4A and 4B), while VE-cadherin levels were significantly reduced (Fig. 4A and 4C), which were both reversed by DGLL pretreatment significantly, indicating that DGLL could inhibit VE-cadherin degradation by inhibiting LPS-induced VE-cadherin phosphorylation (Fig. 4).

5. DGLL inhibits LPS-induced down-regulation of tight junction protein in rat lung tissue

In consistent with adhesion junction protein, western blot results proved that the levels of tight junction proteins, including ZO-1, Occludin, and JAM-1 in rat lung tissue were significantly decreased after LPS induction. In the DGLL 60 mg/kg and 120 mg/kg dose groups, the lung tissue tight junction level was significantly higher than that in LPS group (Fig. 5, A-D) which suggested that DGLL could restore LPS-induced pulmonary tight junction proteins degradation.

Discussion

The present study demonstrated that pretreatment with DGLL inhibited LPS-induced ALI in rats, decreased MPO expression and cytokines and adhesion molecules up-regulation in lung tissues. Moreover, DGLL attenuated LPS-induced rat pulmonary edema and increased pulmonary microvascular permeability, and inhibited the degradation of the adhesion junction protein VE-Cadherin and the tight junction proteins ZO-1, Occludin and JAM-1 in rat lung tissues.

Recent studies have shown that the damage of the pulmonary microvascular barrier and the resulting increased microvascular permeability of pulmonary edema were the main pathological lesions and pathological basis in the early stages of ALI, and was the key point to the treatment of ALI/ARDS.

Epidemiological studies revealed that LPS, a major component of the cell wall of gram-negative bacteria, was the most common cause of lung injury and widely used to establish animal ALI model [10]. Studies have shown that LPS activates nuclear factor-kappa B (NF-κB) by binding to leukocyte toll-like receptor-4 (TLR-4) receptors, inducing a variety of inflammatory factors such as TNF-α, IL-1β, and IL-6, etc., which lead to the destruction of paracellular junctions. At the same time, by inducing the expression of endothelial cell adhesion molecules, LPS can also cause the adhesion of leukocyte to the microvascular endothelium. Adherent leukocytes indirectly damaged the microvessels by releasing proteases and peroxides, causing increased pulmonary microvascular permeability and lung edema, eventually leading to reduced lung compliance and functional impairment [11]. Our previous pharmacological studies have confirmed that diammonium glycyrrhizinate could reduce lung injury by reducing inflammation of the respiratory tract, inhibiting the protein and mRNA levels of inflammatory factors in the lung tissue, and mitigating the expression and activation of NF-κB, which was consistent with others [12, 13]. The present study further confirmed that DGLL can dose-dependently inhibit LPS-induced lung tissue inflammatory cell infiltration, reduce the upregulation of leukocyte infiltration marker MPO levels, as well as reduce the inflammatory cytokines TNF-α and IL-1βand adhesion molecule ICAM-1 levels in lung tissue. These results indicated that DGLL could inhibit the increase of pulmonary microvascular permeability by inhibiting the excessive activation of leukocytes in LPS-induced lung tissue.

In addition to indirectly damaging blood vessels through leukocyte hyperactivation, LPS can also directly damage the microvascular barrier function, resulting in increased microvascular permeability and pulmonary edema [14, 15]. The results of this study demonatrated that the lung wet-to-dry weight ratio, the BALF protein content, and the extravasation of EB in lung tissue in the DGLL pretreatment group were significantly lower than those in LPS group, confirming that DGLL can inhibit LPS induced pulmonary microvascular hyperpermeability and pulmonary tissue edema. The microvascular barrier was mainly regulated by tight junctions and adhesive junctions between microvascular endothelial cells. Adherent junctions were primarily formed from the VE-cadherin protein through the formation of homodimers and were linked to laminin proteins in the cytoplasm and cytoskeletal proteins. Tight junction proteins mainly include Claudin, Occludin, and JAM proteins, which play a role in stabilizing cell indirect tight interactions by linking with the ZOs family of proteins in the cytoplasm [16]. Our study demonstrated that DGLL can significantly inhibit LPS-induced phosphorylation of VE-cadherin in the pulmonary microvasculature on the one hand, thereby significantly inhibiting the degradation of VE-cadherin after LPS induction. On the other hand, DGLL can also stabilize the lung microvascular tight junction proteins Occludin and JAM-1 levels by increasing the expression of ZO-1 protein. DGLL regulated microvascular barriers in lung tissue by simultaneously increasing the expression of tight junction proteins and adhesion proteins in microvascular endothelial cells, thereby inhibiting LPS-induced pulmonary microvascular hyperpermeability and pulmonary tissue edema. However, the regulation mechanism of DGLL on tight junction proteins and adhesion proteins in microvascular endothelial cells still needs further investigation.

Conclusions

In conclusion, DGLL had a significant inhibitory effect on LPS-induced ALI in rats, and its mechanism of action was related to inhibition of inflammatory cell infiltration and degradation of intercellular junction proteins. The result provided a new theoretical basis for the clinical treatment of ALI by DGLL.

Methods

1. Animals and Drugs

Male Spague-Dawlay (SD) rats weighing 180-200 g were provided by Anhui Medical University Experimental Animal Center (Wan Yi Shi Dong Zhun No. 01). Animals were fed with standard grain forage at room temperature 18~22 ℃ for 1 week before experiment. All animals were handled according to the guidelines of the Anhui Medical University Animal Research Committee. The protocols were approved by the Committee on the Ethics of Animal Experiments of the Anhui Medical University (IACUC20180724-18).

DGLL enteric-coated capsules were provided by Jiangsu Zhengda Datianqing Pharmacy Co. Ltd.

2. Experimental protocol

SD rats were randomly divided into 5 groups: sham group (Sham), LPS group, DGLL 30 mg/kg+LPS (DGLL 30+LPS) group, DGLL 60 mg/kg+LPS (DGLL 60+LPS) group and DGLL 120 mg/kg+LPS (DGLL 120+LPS) group. In Sham group, saline (5 ml/kg) was intraperitoneally injected, and physiological saline (5 ml/kg) was given intragastrically 1 hour before saline injection. In LPS group, LPS (10 mg/kg) was injected intraperitoneally, and physiological saline (5 ml/kg) was given intragastrically 1 hour before LPS injection. In DGLL pre-treatment groups, DGLL (30, 60 and 129 mg/kg) which dissolved in physiological saline was intragastrically administered, respectively, 1 hour before LPS injection.

3. Histology and immunohistochemistry examination

3.1 HE staining

Six hours after LPS stimulation, the rats were anesthetized and the lung right middle lobe was cut and fixed in 4% paraformaldehyde, processed for paraffin section (5 μm). Hematoxylin and eosin (HE) staining was conducted to evaluated lung tissue injury.

3.2 MPO immunohistochemical staining

MPO expression in lung tissues was determined by Immunohistochemistry. Briefly, after heat mediated antigen retrival and hydrogen peroxide blockage, the sections were blocked with 5% BSA, incubated overnight with rabbit MPO polyclonal primary antibody (1:200, Abcam, Cambridge, UK) at 4 ℃. And then, the sections were incubated with biotinylated anti-rabbit IgG-HRP at room temperature for 30 min, and

revealed using the DAB substrate kit. The location and expression of MPO-positive cells in lung tissue samples was observed under light microscope.

4. ELISA

Six hours after LPS stimulation, the rats were anesthetized and the lung right middle lobe was taken. The contents of TNF-α and IL-1β in the lung tissue were measured using an ELISA kit (R&D) according to the instructions.

5. Determination of lung dry-wet weight ratio

Six hours after LPS stimulation, the rats were anesthetized and about 100 mg of lung tissue was taken from the right upper lobe. The wet weight was weighed and dried in a vacuum oven at 80 °C for 48 hours to constant weight. The dry weight was weighed and the ratio of wet weight to dry weight of lung tissue was calculated.

6. Pulmonary microvascular permeability test

Six hours after intraperitoneal injection of LPS, rats were injected with 2% EB solution (30 mg/kg) via jugular vein. After 30 min, the rats were sacrificed by carotid artery excision and part of the left lower lobe tissue was taken, weighed, and placed in a clean centrifuge tube. About 100 mg wet lung weight was added to 1ml formamide, 37 °C water bath for 24 hours, centrifuged at 3000 rpm/min for 30 min, and the supernatent was extracted. Absorbance values were measured with a spectrophotometer at a wavelength of 620 nm. The standard curve method was used to calculate the EB content of each sample. Pulmonary microvascular permeability was expressed as the ratio of EB content to lung wet weight.

7. Determination of protein concentration in BALF

Six hours after intraperitoneal injection of LPS, the rats were anesthetized and a plastic cannula was inserted into the trachea to collect BALF by sterile physiological saline aspiration for 3 times. The BALF sample was centrifuged (1300 *g*, 4 °C) for 10 min and the supernatant was extracted. BCA method was used to detect total protein concentration in BALF.

8. Western blot analysis

Six hours after LPS stimulation, the rats were anesthetized and the right lower lobe was taken. One-step RIPA method was used to extract total protein of lung tissue and protein concentration was measured according to BCA method. After SDS-PAGE electrophoresis, transfer membrane, blocking, the following protein content was detected. The primary antibodies and concentrations used were: ICAM-1 (1:1000, Cell Signaling Technology), phospho-VE-Cadherin (1:1000, Abcam), VE-cadherin (1:500, Santa Cruz), ZO-1 (1:1000, Invitrogen), Occludin (1:500, Invitrogen), JAM-1 (1:1000, Santa Cruz), and GAPDH (1:5000, Cell Signaling Technology). After reacting with the corresponding secondary antibody, the band was luminescently displayed by ECL. GAPDH was used as an internal reference. The average optical density of the Western bands was measured using the Quantity One image analyzer software (Bio-Rad, Richmond, CA, USA), and the ratio of the average optical density of the target band to the corresponding GAPDH was calculated. The results are expressed as the ratio with respect to Sham group.

9. Statistical analysis

All data were expressed as mean ± SE. One-way ANOVA and Turkey tests were performed by using SPSS 15.0 mathematical statistics software. $P<0.05$ was considered significant.

Declarations

Ethics approval and consent to participate

All animals were handled according to the guidelines of the Anhui Medical University Animal Research Committee. The protocols were approved by the Committee on the Ethics of Animal Experiments of the Anhui Medical University (IACUC20180724-18).

Consent for publication

Not applicable.

Competing interests

The authors declare no competing interests.

Funding

This work was supported financially by the Key Projects of Natural Science Research of Anhui Province [KJ2016A374].

Authors' contributions

M.M.L performed and funded the research, and analyzed the data; J.Z. and D.J contributed to animal experiments; J.Y. and Y.P.H contributed to immunochemistry analysis; Q.W designed the research,

interpreted the data, wrote the manuscript, and finally approved the submission of this manuscript. All authors have read and agreed with the manuscript.

Acknowledgements

Not applicable.

Availability of data and material

All data generated or analyzed during this study are included in this published article.

Abbreviations

ALI, acute lung injury; ARDS, acute respiratory distress syndrome; BALF, bronchoalveolar lavage fluid; DGLL, diammonium glycyrrhizinate lipid ligand; EB, evans blue; HE, hematoxylin and eosin; LPS, lipopolysaccharide; MPO, myeloperoxidase; NF-κB, uclear factor-kappa B; SD, Spague-Dawlay; TPG, Tianqing Ganping; TLR-4, toll like receptor-4.

References

1. Bellani G, Laffey JG, Pham T, Fan E, Brochard L, Esteban A, Gattinoni L, van Haren F, Larsson A, McAuley DF, Ranieri M, Rubenfeld G, Thompson BT, Wrigge H, Slutsky AS, Pesenti A; LUNG SAFE Investigators; ESICM Trials Group. Epidemiology, patterns of care, and mortality for patients with acute respiratory distress syndrome in intensive care units in 50 countries. JAMA. 2016;315:788-800.
2. Meduri GU, Headley AS, Golden E, Carson SJ, Umberger RA, Kelso T, Tolley EA. Effect of prolonged methylprednisolone therapy in unresolving acute respiratory distress syndrome: a randomized controlled trial. JAMA. 1998;280:159-65.
3. Matthay MA, Zimmerman GA. Acute lung injury and the acute respiratory distress syndrome: four decades of inquiry into pathogenesis and rational management. Am J Respir Cell Mol Biol. 2005;33:319-27.
4. Johnson ER, Matthay MA. Acute lung injury: epidemiology, pathogenesis, and treatment. J Aerosol Med Pulm Drug Deliv. 2010;23:243-52.
5. He Y, Lou X, Jin Z, Yu L, Deng L, Wan H. Mahuang decoction mitigates airway inflammation and regulates IL-21/STAT3 signaling pathway in rat asthma model. J Ethnopharmacol. 2018;224:373-80.
6. Zhong Y, Zhou J, Liang N, Liu B, Lu R, He Y, Liang C, Wu J, Zhou Y, Hu M, Zhou J. Effect of Maxing Shigan Tang on H1N1 Influenza A Virus-Associated Acute Lung Injury in Mice. Intervirology. 2016;59:267-74.
7. Yao L, Sun T. Glycyrrhizin administration ameliorates Streptococcus aureus-induced acute lung injury. Int Immunopharmacol. 2019;70:504-11.
8. Chen J, Zhang W, Zhang L, Zhang J, Chen X, Yang M, Chen T, Hong J. Glycyrrhetinic acid alleviates radiation-induced lung injury in mice. J Radiat Res. 2017;58:41-7.

9. Zhang D, Liu B, Cao B, Wei F, Yu X, Li GF, Chen H, Wei LQ, Wang PL. Synergistic protection of Schizandrin B and Glycyrrhizic acid against bleomycin-induced pulmonary fibrosis by inhibiting TGF-β1/Smad2 pathways and overexpression of NOX4. Int Immunopharmacol. 2017;48:67-75.
10. Chen H, Bai CX, Wang XD. The value of the lipopolysaccharide-induced acute lung injury model in respiratory medicine. Expert Rev Resp Med. 2010;4:773-83.
11. Abraham E. Neutrophils and acute lung injury. Crit Care Med. 2003;31:S195-99.
12. Feng C, Wang H, Yao C, Zhang J, Tian Z. Diammonium glycyrrhizinate, a component of traditional Chinese medicine Gan-Cao, prevents murine T-cell-mediated fulminant hepatitis in IL-10- and IL-6-dependent manners. Int Immunopharmacol. 2007;7:1292-8.
13. Jin J, Xiong T, Hou X, Sun X, Liao J, Huang Z, Huang M, Zhao Z. Role of Nrf2 activation and NF-κB inhibition in valproic acid induced hepatotoxicity and in diammonium glycyrrhizinate induced protection in mice. Food Chem Toxicol. 2014;73:95-104.
14. Dreymueller D, Martin C, Kogel T, Pruessmeyer J, Hess FM, Horiuchi K, Uhlig S, Ludwig A. Lung endothelial ADAM17 regulates the acute inflammatory response to lipopolysaccharide. EMBO Mol Med. 2012;4:412-23.
15. Veszelka S, Pásztói M, Farkas AE, Krizbai I, Ngo TK, Niwa M, Abrahám CS, Deli MA. Pentosanpolysulfate protects brain endothelial cells against bacterial lipopolysaccharide-induced damages. Neurochem Int. 2007;1:219-28.
16. Mehta D, Malik AB. Signaling mechanisms regulating endothelial permeability. Physiol Rev. 2006;86:279-367.

Figures

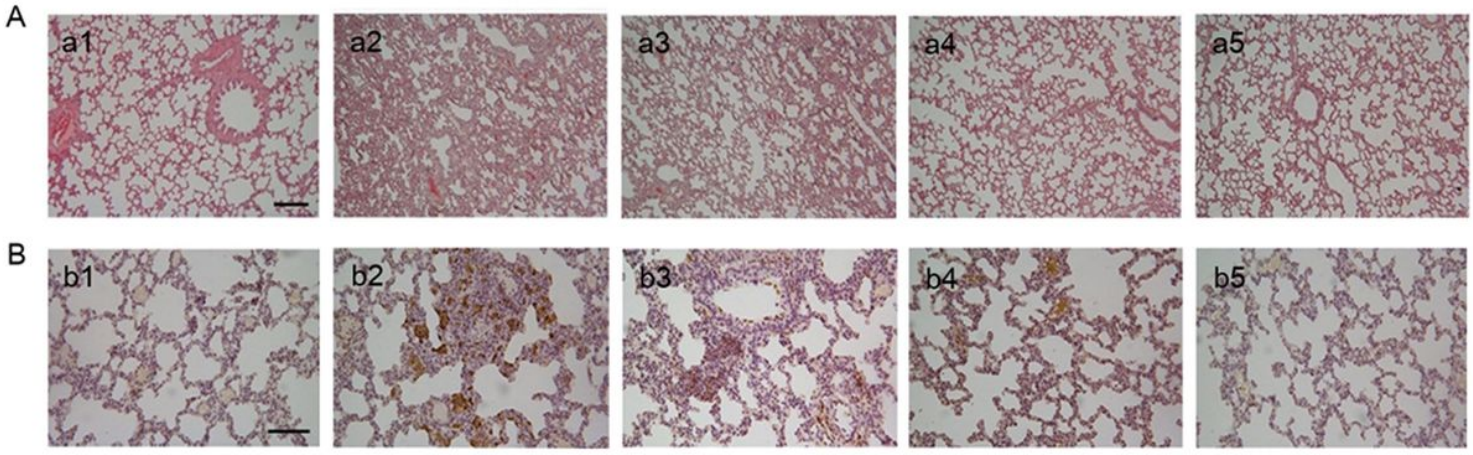

Figure 1

The effect of DGLL on acute lung tissue injury and MPO expression in lung tissue after LPS stimulation. A, representative HE staining images of the lung tissues in Sham group (a1), LPS group (a2), DGLL

30+LPS group (a3), DGLL 60+LPS group (a4) and DGLL 120+LPS group (a5) under 4 x objective lens, bar = 200 μm; B, representative MPO immunohistochemical staining images of the rat lung tissue in Sham group (b1), LPS group (b2), DGLL 30+LPS group (b3), DGLL 60+LPS group (b4) and DGLL 120+LPS group (b5) under 10 x objective lens, bar = 200 μm.

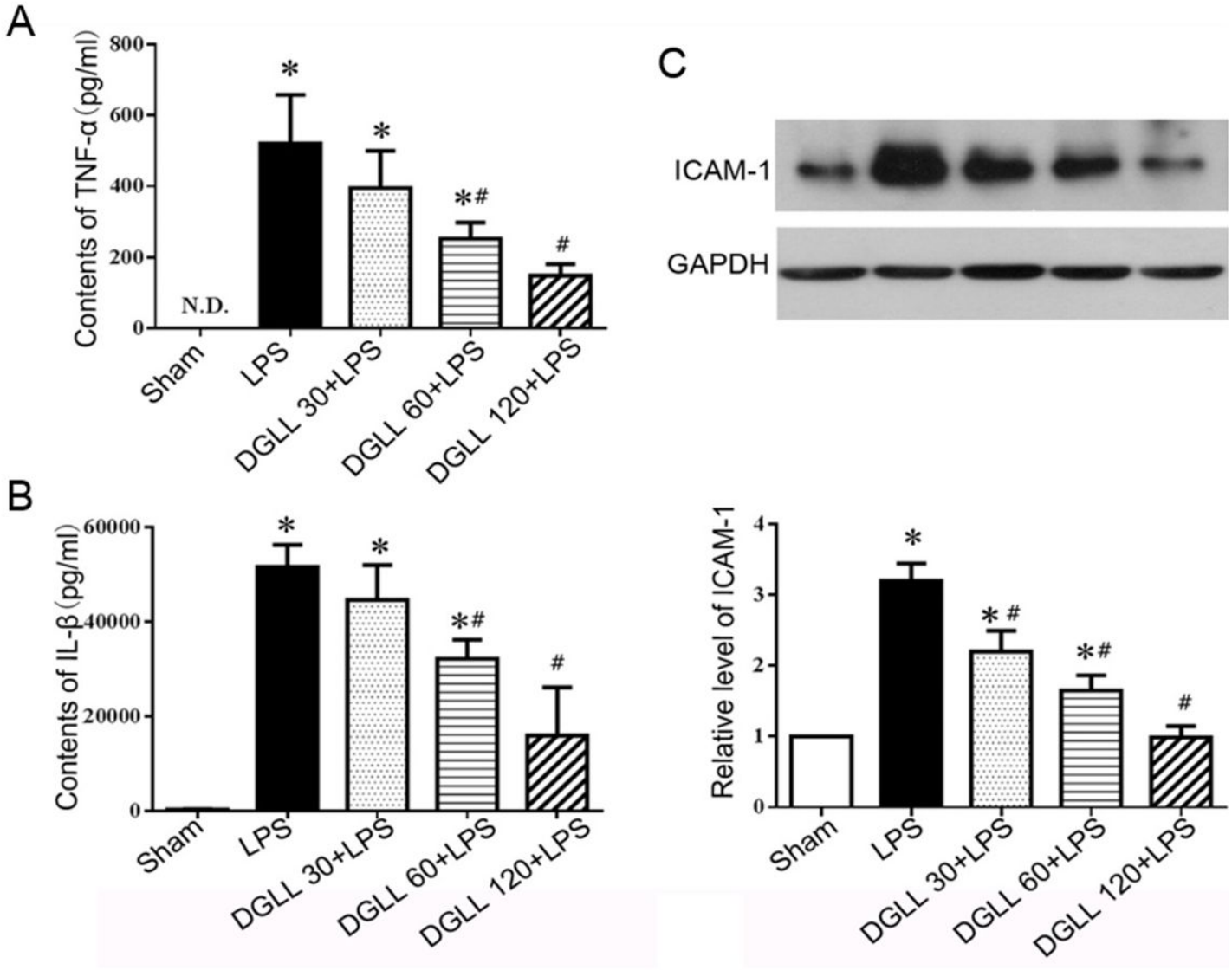

Figure 2

The effect of DGLL on upregulation of inflammatory cytokines and adhesion molecules induced by LPS. A and B, statistical analysis for expression of TNF-α (A) and IL-1β (B) in the rat lung tissues detected by ELISA; C, Representative Western blot image and statistical analysis of ICAM-1 level in rat lung tissues. *, $P<0.05$ vs Sham group; #, $P<0.05$ vs LPS group.

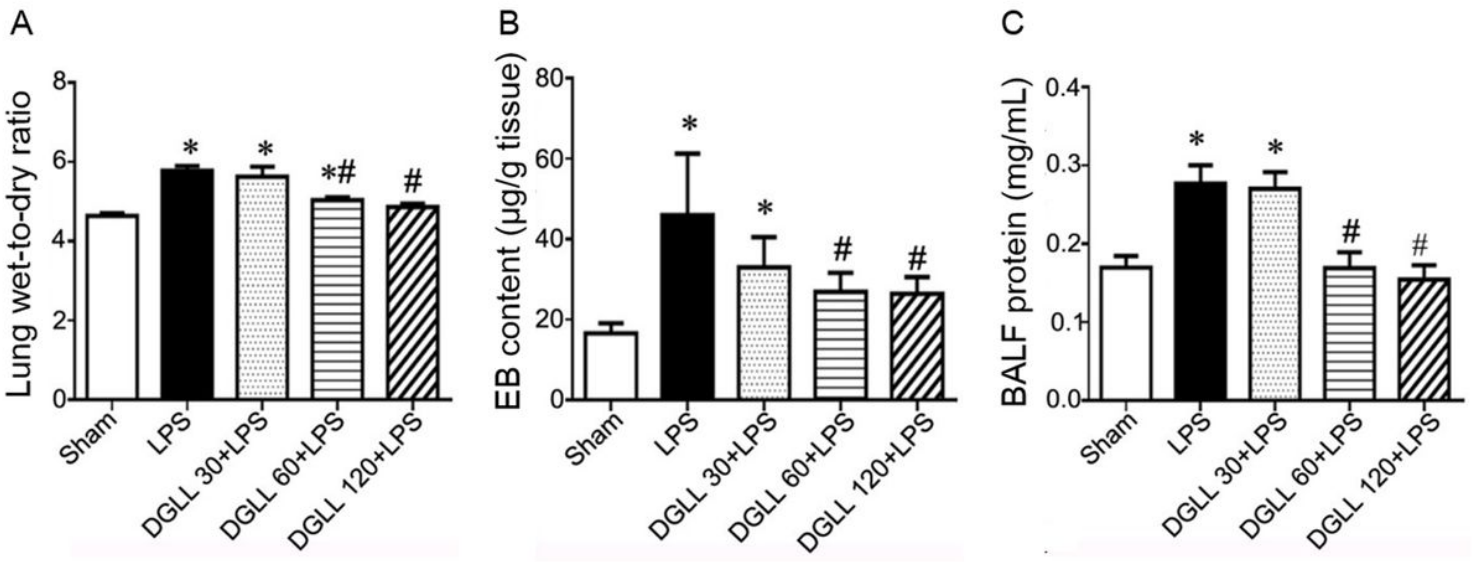

Figure 3

The effect of DGLL on pulmonary microvascular permeability and pulmonary tissue edema induced by LPS. *, P<0.05 vs Sham group; #, P<0.05 vs LPS group.

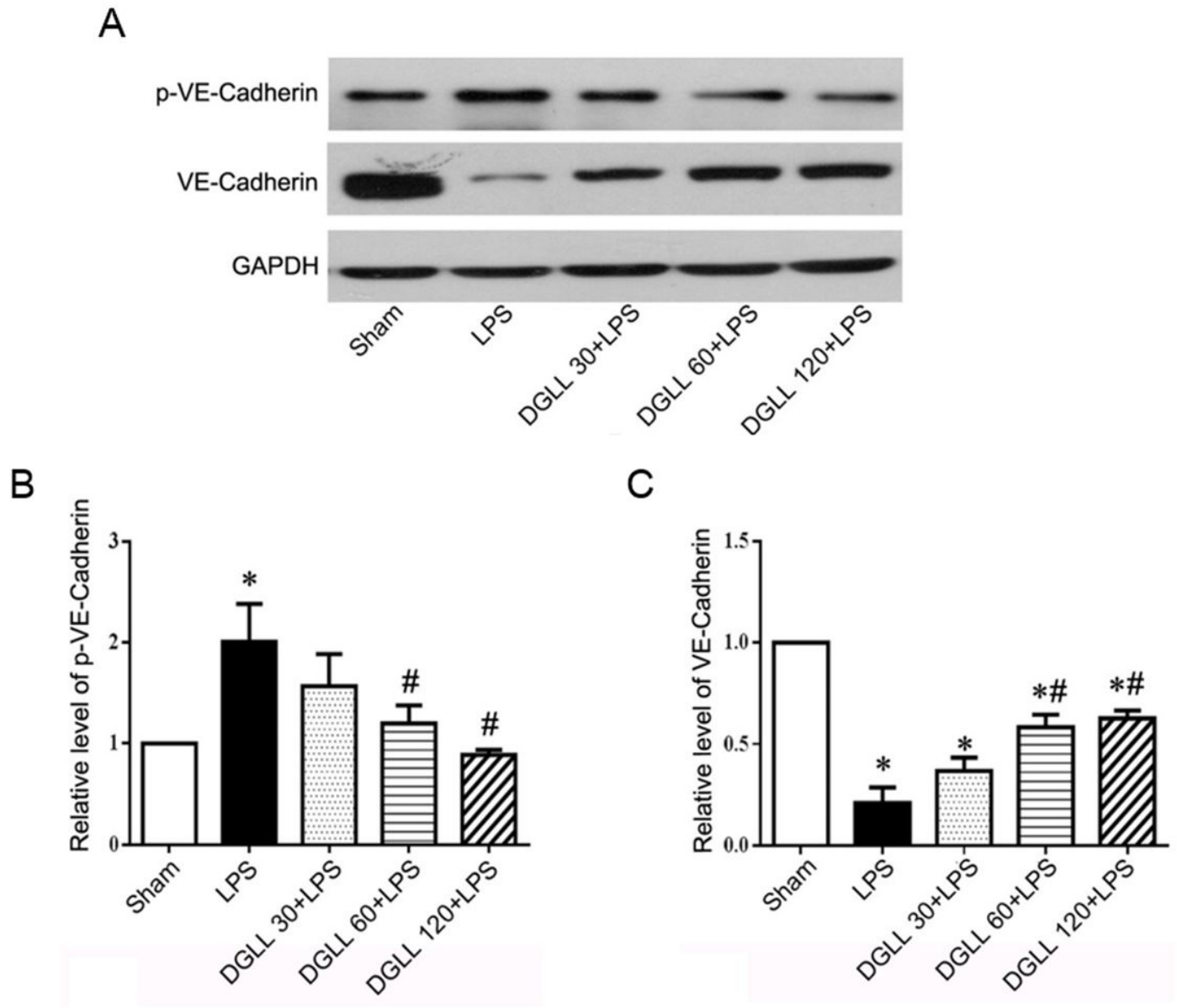

Figure 4

The effect of DGLL on phosphorylation and degradation of rat lung tissue adhesion junction protein VE-Cadherin caused by LPS. A, Representative Western blot image of p-VE-Cadherin and VE-Cadherin. B and C, statistical analysis of p-VE-Cadherin (B) and VE-Cadherin (C) level in rat lung tissues. *, P<0.05 vs Sham group; #, P<0.05 vs LPS group.

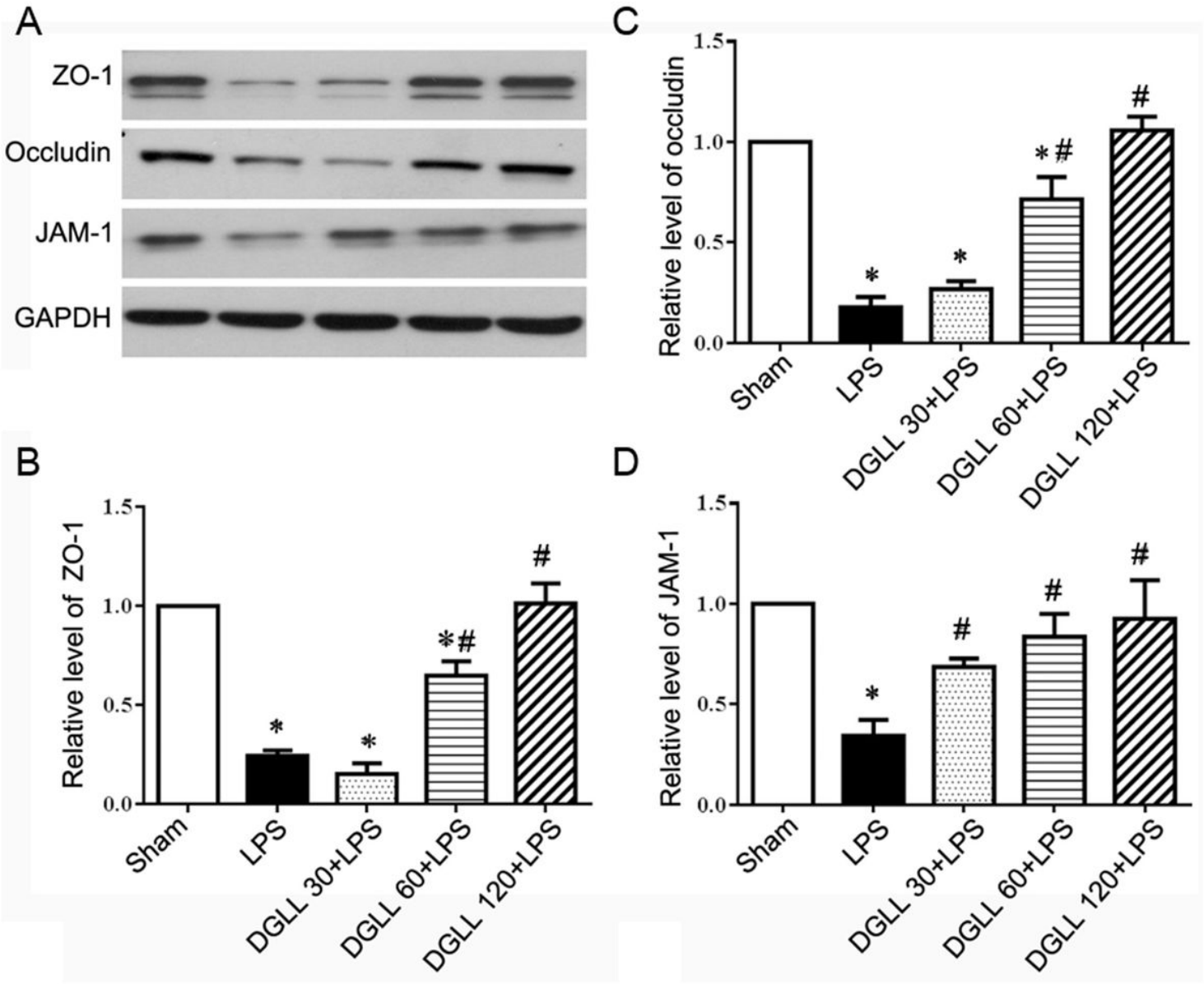

Figure 5

The effect of DGLL on the down-regulation of tight junction proteins levels in rat lung tissues caused by LPS. A, Representative Western blot image of ZO-1, Occludin and JAM-1. B-D, statistical analysis of ZO-1 (B), Occludin (C) and JAM-1 (D) level in rat lung tissues, respectively. *, $P<0.05$ vs Sham group; #, $P<0.05$ vs LPS group.